Arch. Metall. Mater. **67** (2022), 1, 147-154

DOI: https://doi.org/10.24425/amm.2022.137483

D. PELCZAR[1], P. DŁUGOSZ[2], P. DARŁAK[2], A. SZEWCZYK-NYKIEL[1], M. NYKIEL[1], M. HEBDA[1*]

THE EFFECT OF BN OR SiC ADDITION ON PEO PROPERTIES OF COATINGS FORMED ON AZ91 MAGNESIUM ALLOY

Currently, due to the economic and ecological aspects, light alloys are increasingly important construction material, in particular in the transport industry. One of the popular foundry magnesium alloys is the alloy AZ91, which among others due to mechanical properties and technological features, is used, for example, for light structural parts.

The paper presents the results of research on modification of the AZ91 alloy surface layer in the plasma electrolytic oxidation process. The change of usable properties of the produced coatings was obtained by introducing additions of silicon carbide or boron nitride. The thickness and hardness of the protective layers produced, resistance to scratches and corrosion resistance were determined. Moreover, the friction coefficient of the coating-steel pair was investigated. The quality of the connections made between the coating and the substrate, i.e. the magnesium alloy, was also evaluated. The results obtained for coatings with silicon carbide or boron nitride additives were always compared to the results obtained for unmodified samples.

On the basis of the obtained results, it was shown that the introduction of boron nitride additive to the AZ91 alloy coating produced in the plasma electrolytic oxidation process significantly improves the resistance to: (i) corrosion and (ii) abrasive wear of the coating.

Keywords: composite oxide film; abrasive wear resistance; corrosion behavior; scratch resistance; protective coatings

1. Introduction

The progress of civilization is manifested, inter alia, in the continuous improvement of manufacturing technology and the development of new, innovative materials. It is also one of the factors increasing people's awareness, among others in the scope of: (i) environmental protection, e.g. by reducing greenhouse gas emissions during the manufacture or operation of products, (ii) searching for alternative solutions to reduce the use of non-renewable energy sources and raw materials, and (iii) technologies aimed at waste-free manufacturing of products with considering their recycling. These economic and ecological aspects are of particular importance in the broadly understood transport industry. For this reason, in recent years, many scientific centers have been conducting intensive research on the modification of light alloys, among others on the magnesium matrix. Magnesium alloys allow for a significant reduction in the weight of components, e.g. in comparison to standard steel products, while maintaining excellent strength properties [1]. This advantage is extremely important, especially in constructions, which are expected to significantly reduce the cost of fuel consumption, including airplanes, spacecraft or public utility vehicles [2,3]. In addition, magnesium alloys also exhibit biocompatibility, useful in medical applications [2]. On the other hand, it is a material that tends to corrode under certain conditions. This effect is particularly observable when the material is exposed in moist and polluted air since the oxide layer formed on the surface is then leaky. In addition, magnesium generally corrodes in an environment of pH <10.5. That is why numerous studies have been conducted to increase its usefulness, among others by applying protective coatings.

Such coatings can combine the functions of both effective magnesium protection against corrosion and increased wear resistance, e.g. abrasive. It is important that the coating produced on the surface of the alloy is characterized by uniformity, continuity, non-porous and good cohesion with the substrate. The materials of some of the new generation coatings may also exhibit the so-called ability to self-healing. Until recently, the most common

[1] CRACOW UNIVERSITY OF TECHNOLOGY, FACULTY OF MATERIALS ENGINEERING AND PHYSICS, DEPARTMENT OF MATERIALS ENGINEERING, 24 WARSZAWSKA STR., 31-155 KRAKOW, POLAND
[2] CENTRE OF CASTING TECHNOLOGY, RESEARCH NETWORK LUKASIEWICZ-KRAKOW INSTITUTE OF TECHNOLOGY, ZAKOPIAŃSKA 73, 30-418 KRAKOW, POLAND
* Corresponding author.mhebda@pk.edu.pl

way to protect magnesium against corrosion was: (i) applying metallic galvanic coatings (e.g. chrome plating, nickel plating) or (ii) coating with conversion coatings (e.g. phosphate) [4]. These methods are very well known and provide relatively good corrosion protection. However, it should be remembered that regardless of the type of coating produced, the process of applying such a layer should be relatively inexpensive and safe for both people and the environment. These aspects constitute the greatest disadvantage of the aforementioned methods of applying protective coatings. That is why in recent years there has been a rapid development in the world of issues related to surface engineering aimed at developing alternative, more secure processes that enable the production of effective protection barriers among others on magnesium alloys [5,6]. One of the more developing techniques that allow the formation of coatings on metals that are a dielectric oxide layer [7] and the modification of their surface is Plasma Electrolytic Oxidation (PEO). This process is also called Plasma Anodizing (PA) or Micro Arc Oxidation (MAO) [8].

The plasma oxidation technology is based on a similar principle to the classical anodizing process, but it uses high voltage up to a thousand volts. In addition, in both processes the oxidized object is an anode immersed in the electrolyte but with the difference that acid electrolyte is used for classical anodizing, while alkaline electrolyte during the plasma oxidation. The electrolyte must be continuously cooled during the process due to the exothermic nature of the process. The overheating of the electrolyte may result in cracking of the oxide coating produced. It is also recommended to continuously mix the electrolyte in order to maintain a constant concentration of ions in the entire electrolyte volume. Proper selection of the parameters of the entire process allows the creation of a ceramic coating coherent with the substrate, which is characterized by high hardness and decorative functions. In addition, they are homogeneous and resistant to galvanic corrosion [2,9,10]. The process of plasma oxidation was developed to remove, among other defects and imperfections of classical anodizing. The most important of them is the possibility of producing much thicker coatings and modifying their composition and thus their properties. Another advantage of PEO is the reduction of the number of processes preceding the stage of the coating production itself. In the case of plasma oxidation, the purification of the layer is limited to decreasing, which allows saving both time and the amount of equipment necessary to carry out the processes compared to classical anodizing. Based on the available research results, it is possible to predict the influence of the applied PEO process parameters on the properties and morphology of the coatings produced on magnesium, aluminum or titanium alloys [11-15]. There is also information on the influence of the structure and concentration of individual magnesium alloy components on the properties of protective layers obtained in the PEO process [16-18]. On the other hand, limited information can be found on the materials in which PEO coatings were modified with additives [19-23] during production. The development of such a technology can be important both in order to improve the anti-corrosion and tribological properties of alloys. The research results presented in the article concern the impact of the use of boron nitride (BN) or silicon carbide (SiC) additives, introduced into the electrolyte composition, on the morphology, anti-corrosion and tribological properties of coatings made on the AZ91 alloy in the PEO process.

2. Materials and Methods

The PEO process was carried out on an AZ91 magnesium alloy containing: Al 8.10 ÷ 9.30 wt.%, Zn 0.40 ÷ 1.00 wt.%, Mn 0.17 ÷ 0.35 wt.%. Cylindrical samples with dimensions: 25.4 × 5 mm were used for the tests. Prior to the PEO process, magnesium alloy specimens were ground and polished using successive grades of SiC coated abrasive papers up to 1200 grit to achieve a smooth surface. Next, samples were cleaned, in acetone for 10 min, ultrasonically, then washed in distilled water and finally rinsed in alcohol. The aqueous electrolyte solution contained $Na_2SiO_3x5H_2O$. The modified electrolytes were prepared by adding 5 g/L BN or SiC particles with an average diameter of 2 μm and 3 μm, respectively to the base electrolyte. The volume fraction of BN or SiC added to the electrolyte was 0.14 vol.% and 0.93 vol.% respectively. A PEO treatment electrolyte without the BN or SiC particles was utilized as a reference. During the PEO process, the samples and the wall of the stainless steel container were used as the anode and the cathode, respectively. A constant current density was maintained at 5.0 A/dm^2 by modulating the positive and negative voltages. A maximum voltage of 400 V was set for the PEO process. The temperature of the electrolyte solution was always kept at ambient temperature by a cooling system. After the PEO treatment, each coated sample was washed thoroughly in distilled water and dried in the air immediately.

The designation of the samples used in the tests, depending on the method of their preparation, is presented in TABLE 1.

TABLE 1

The designation of the samples used in tests depending on the type of coating applied

No	Sample designation	The type of coating
1	AZ91	No coating
2	PEO AZ91	Coating made in PEO process on the AZ91 alloy
3	PEO AZ91 SiC	Coating with the addition of SiC, made in the PEO process on the AZ91 alloy
4	PEO AZ91 BN	Coating with the addition of BN, made in the PEO process on the AZ91 alloy

The cross-sectional morphologies of coatings were examined using the scanning electron microscope (SEM, JSM5510LV).

The potentiodynamic polarization tests were performed using ATLAS 0531 UI&IA potentiostat cooperating with AtlasCorr05 software. Measurements were carried out in the environment of a 3.5% NaCl solution at an ambient temperature according to the methodology described in [24].

Roughness measurement was performed by using the Mitutoyo Surftest SJ-301 profilometer. The measurement was made on a distance of 350 μm. The pressure of the head on the analysis material was 0.75 mN. The moving speed of the head was 0.5 mm/s. Five tests were carried out for each of the samples tested.

Microstructural observations were conducted using a Nikon Eclipse ME600 optical microscope with digital image recording.

The dry sliding wear properties of materials were investigated using a ball-on-disk friction method. The T-01M device was used and two different rotational speeds of the disk – 0.2 m/s and 0.02 m/s. For each measurement, the friction distance was 500 m, and the applied load was 10 N. As a counter-sample a 1.3505 bearing steel ball, with a 6 mm diameter, was used.

The hardness test was carried out using the Rockwell method, on the F scale (using the Innovatest 600 MBDL device). While HV1 microhardness measurements were made using the Innovatest 400 device. Ten measurements were done for each variant of the sample.

The assessment of the adhesion of the coating to the substrate and its resistance to scratches in the micro-scale was made using a scratch test (using the MST^3 device, Anton Paar). During the measurement, the pressure of the diamond indenter increased in a linear manner from 0.5 N to 5 N, at a rate of 4 N/min. The test was carried out on a 5 mm distance. The following parameters were registered: normal force, acoustic emission, and penetration depth.

3. Results and Discussion

All coatings produced in the PEO process were characterized by a good adhesion-diffusion bond with the substrate. The obtained coatings uniformly covered the surfaces of the samples and were homogeneous. Their thickness was about 10 μm, which was presented on representative areas of the coatings of the samples designated as PEO AZ91 and PEO AZ91 BN (Fig. 1).

What is important, the coating surface, regardless of its variant, was characterized by a fine and homogeneously distributed porosity (Fig. 2). Thanks to this, it creates a compact barrier that protects the base material against the impact of the environment.

Obtained results indicate a lack of significant influence of BN or SiC additives added to the electrolyte composition on: (i) the PEO process and (ii) the quality of the coatings produced. Moreover, they confirm that the oxidation process was carried out correctly. Coatings of similar morphology obtained in their research, among others Wang et al. [13].

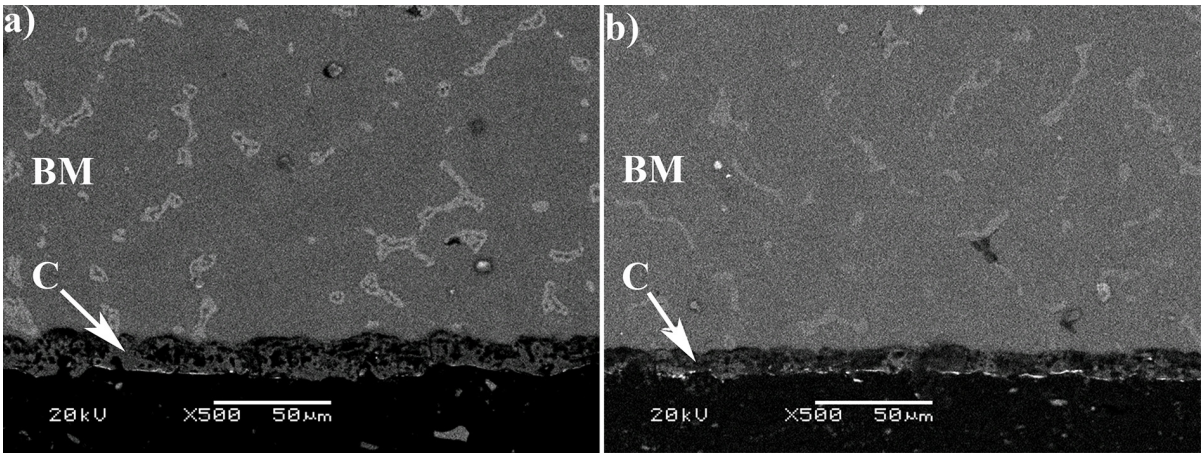

Fig. 1. Cross-section microstructures of sample: a) PEO AZ91, b) PEO AZ91 BN. BM – base material, C – coating

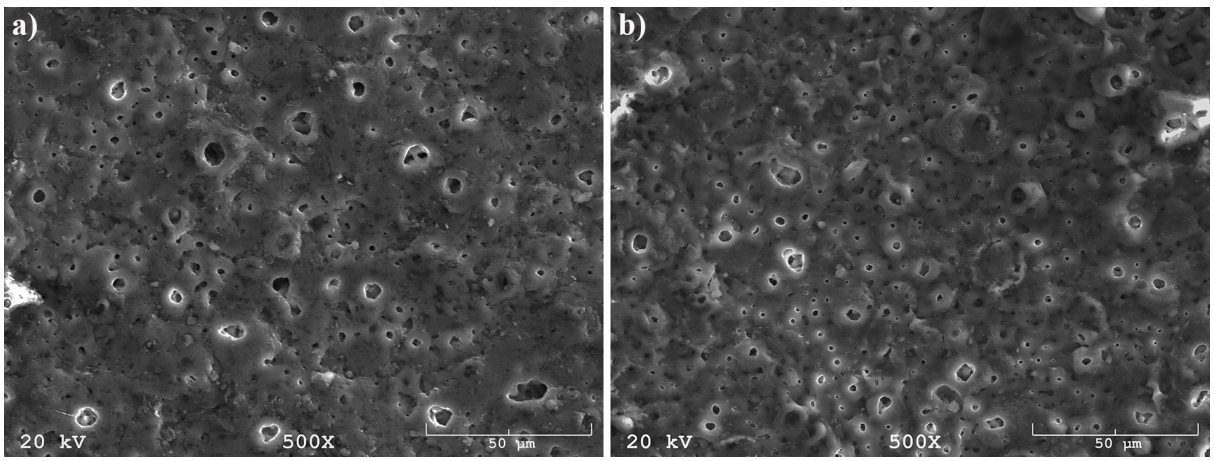

Fig. 2. Surface morphology of the PEO coating modified with the addition of: a) BN, b) SiC

The results of roughness measurements of the tested samples are presented in TABLE 2.

TABLE 2

Results of the AZ91 alloy roughness measurement, depending on the type of PEO coating applied and before it was made

No	Sample	Ra [µm]	Rz [µm]	Rq [µm]
1	AZ91	0.55 ± 0.04	3.74 ± 0.59	0.69 ± 0.01
2	PEO AZ91	0.95 ± 0.03	6.78 ± 0.71	1.21 ± 0.08
3	PEO SiC	0.96 ± 0.08	6.74 ± 0.64	1.21 ± 0.04
4	PEO BN	0.97 ± 0.01	6.99 ± 0.76	1.23 ± 0.01

The AZ91 alloy surface prepared for the PEO process was characterized by Ra and Rz parameters. Their values were 0.55µm and 3.74 µm, respectively. Regardless of the electrolyte composition, after the oxidation process, the surface layer of the samples achieved a similar roughness, the Ra coefficient of about 0.96 µm and Rz about 6.8 µm. This quality of the surface can be compared to the material›s roughness, which is obtained after using typical types of chip machining, for example, milling, cutting or drawing. The effect of surface roughness increase after the PEO process is related to the mechanism of coating growth, involving the electro-, thermal-, and plasma-chemical reactions, in particular, the occurrence of micro-porosity on its surface (Fig. 2) [25-28].

Fig. 3 presents the results of measurements of the HRF hardness and microhardness of the AZ91 alloy and samples with the produced protective layers.

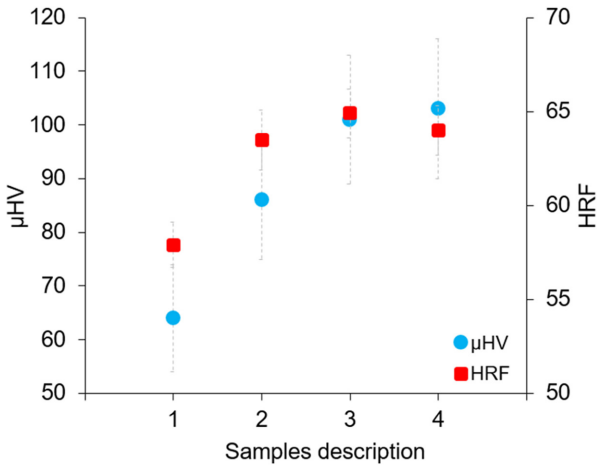

Fig. 3. Hardness and microhardness of the tested materials. Samples designation as described in Table 1

Based on the obtained results, it was found that the nature of registered dependencies of hardness changes on the type of samples tested was similar regardless of the measurement method used. The measured values have unambiguously confirmed that the use of plasma oxidation techniques increases the hardness of the magnesium alloy. In addition, the addition of additives in the form of BN or SiC to the coating allows an additional, about 18%, increase in the hardness of the material, which is particularly evident during microhardness measurements. During HRF measurements the hardness differences are less visible, which is a consequence of using a much larger penetrator and loading force, therefore the substrate affected the result more than oxidized thin surface layer.

Figures 4 and 5 show a comparison of changes in the coefficient of friction depending on the rotational speeds of the disk used, 0.02 m/s and 0.2 m/s respectively.

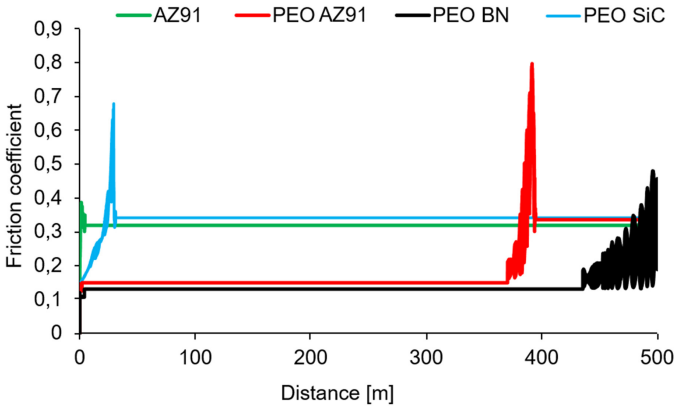

Fig. 4. The friction coefficient as a function of the sliding distance for the AZ91 magnesium alloy (without or with a coating) – steel 1.3505 rubbing pair, using a rotational speed of 0.02 m/s

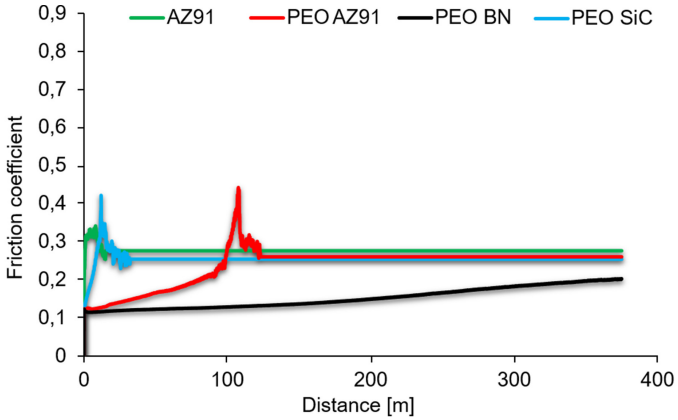

Fig. 5. The friction coefficient as a function of the sliding distance for the AZ91 magnesium alloy (without or with a coating) – steel 1.3505 rubbing pair, using a rotational speed of 0.2 m/s

Based on the recorded results, it was found that the AZ91 magnesium alloy without a protective coating exhibits a similar level of friction coefficient of approx. 0.3, regardless of the rotational speed used. The increase in the coefficient of friction visible on the curves in the initial measuring range is most probably related to the process of piercing and removing the thin oxide layer spontaneously formed on the surface of the magnesium alloy. However, the formation of an oxide coating on the surface of AZ91 alloy in the PEO process allowed for a significant reduction of the coefficient of friction. Values of approximately 0.15 and 0.13 were obtained for the applied speeds of 0.2 m/s and 0.02 m/s, respectively. In addition, it was observed that the change of the coefficient of friction during ball-on-disc tests takes place on the way around 370 m for the speed of 0.02 m/s

and 100 m at the speed of 0.2 m/s. The introduction of SiC or BN additives into coatings made the material tested behave quite differently in the analyzed friction pairs. The presence of the SiC addition in the coating caused a continuous increase of the coefficient of friction from the beginning of the measurement until its stabilization, which followed the movement of about 50 m regardless of the rotational speed used. The observed effect occurring in the initial stage of tests indicates the process of removing the produced coating during the measurement. This is confirmed by the fact that the stabilized value of the coefficient is about 0.3, and is practically identical to the value registered for the reference sample without coating.

On the other hand, the introduction of the BN additive into the PEO coating allowed not only to achieve the lowest friction coefficient among the tested surfaces, amounting to about 0.12 but more importantly its stabilization in practically the entire measuring range. Such an effect indicates very good sliding properties of the coating in conditions of technically dry friction with simultaneously high resistance to damage. During measurements at the rotational speed of 0.02 m/s, rapid changes in the coefficient of friction that may indicate damage to the coating were recorded after the distance of 440 m. However, the use of a speed of 0.2 m/s caused that the coefficient of friction on the distance up to 120 m in a very smooth way began to increase from 0.12 to 0.2, then it will remain stable until the end of the test. This value is still significantly lower than that obtained for the AZ91 magnesium alloy. The friction coefficient of the PEO BN – steel rubbing pair, can be compared to the values recorded in polyethylene – steel systems.

Fig. 6 presents traces of the trajectory of the impact of the rubbing pair, left on the surface of the tested samples after the ball-on-disc tests.

Only samples with PEO BN coating were characterized by negligible damage, in particular when the measurements were carried out at a rotational speed of 0.02 m/s (Fig. 6b). In addition, these samples were the only ones that showed slight weight loss after the tests. On all the other coatings produced, there are clear recesses associated with wiping the material through the counter-sample (Fig. 6c-d). The width of the marks formed is, however, slightly smaller compared to the abrasions visible on the surface of the AZ91 magnesium alloy base sample (Fig. 6a). It was also observed that the use of the speed of 0.02 m/s means that the traces created are irregular in character and additionally depressions are visible on their entire circumference. They testify to the accumulation in the trajectory of the abrasive movement of the material, which is then removed together with the adhesively bonded material. Such effects were not observed at the rotational speed of 0.2 m/s, which allows to state that the acting centrifugal force is so large that it removes abrasive products created on the surface of the material.

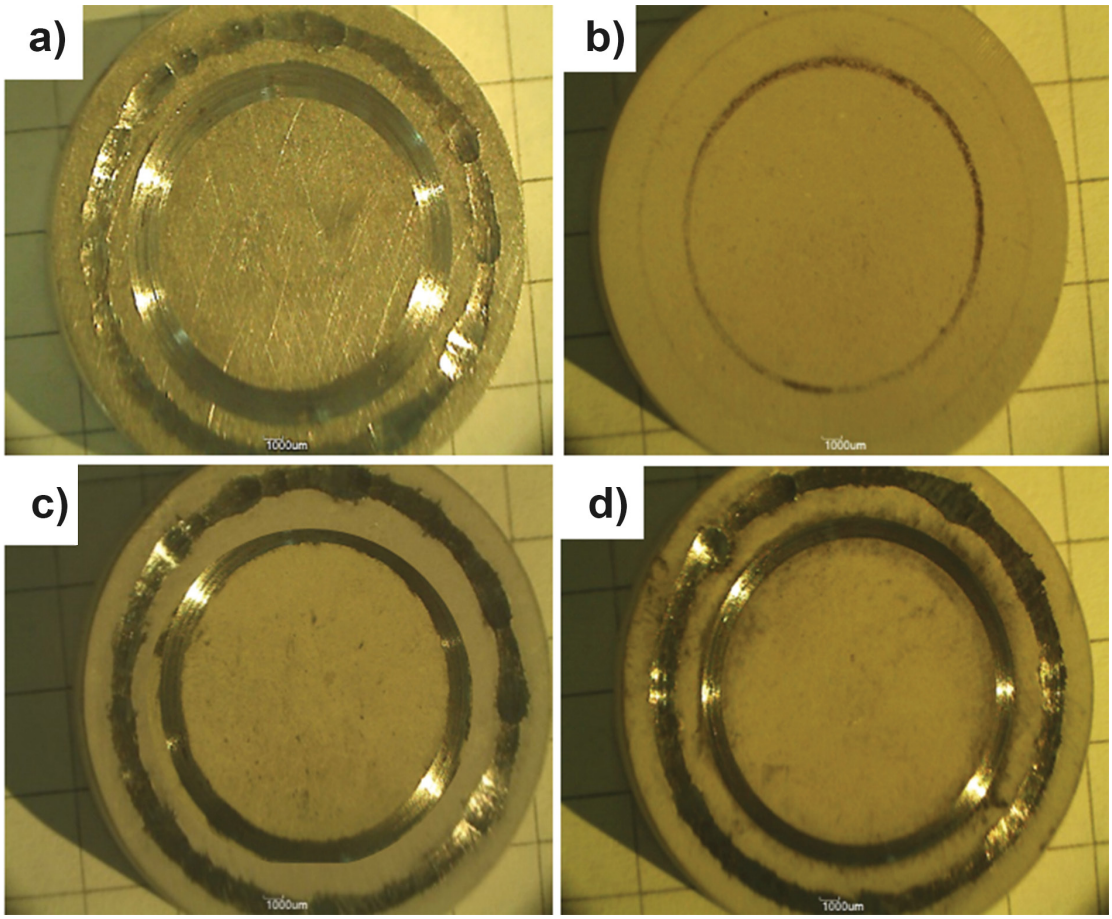

Fig. 6. Traces of the trajectory of counter-sample interaction depending on the rotational speed used: 0.2 m/s – internal trace, 0.02 m/s – external trace for samples a) AZ91, b) PEO BN, c) PEO SiC, d) PEO 10

The assessment of the adhesion quality of the produced PEO coatings to the magnesium alloy was based on the scratch test results. Fig. 7 shows the acoustic emission (EA) change curves and the indentation (Pd) as a function of sliding distance and linear load increase (Fn) for all analyzed samples.

The most straight-line course of acoustic emission was recorded for the unmodified AZ91 alloy. Moreover, the process of sinking the diamond cone into this sample took place almost evenly throughout the whole test. For the remaining samples, regardless of the type of protective coating produced, two characteristic areas can be distinguished on the EA curves: (i) rectilinear, indicating no damage to the coating, and (ii) with an intensely changing amplitude of the measured signal, indicating the break of the surface layer continuity. The pierce of the shell can be read from the Pd curves in the area in which a sudden increase in the penetration depth of the indenter occurs. The recorded scratch test results showed that almost twice the load of the diamond indenter is required to damage the PEO BN coating as compared to the unmodified PEO layer (Fig. 7).

Fig. 8 presents Tafel›s curves of all analyzed samples. It is well known that the corrosion potential (*Ecorr*) is related to the thermodynamic feature, presenting the corrosion tendency,

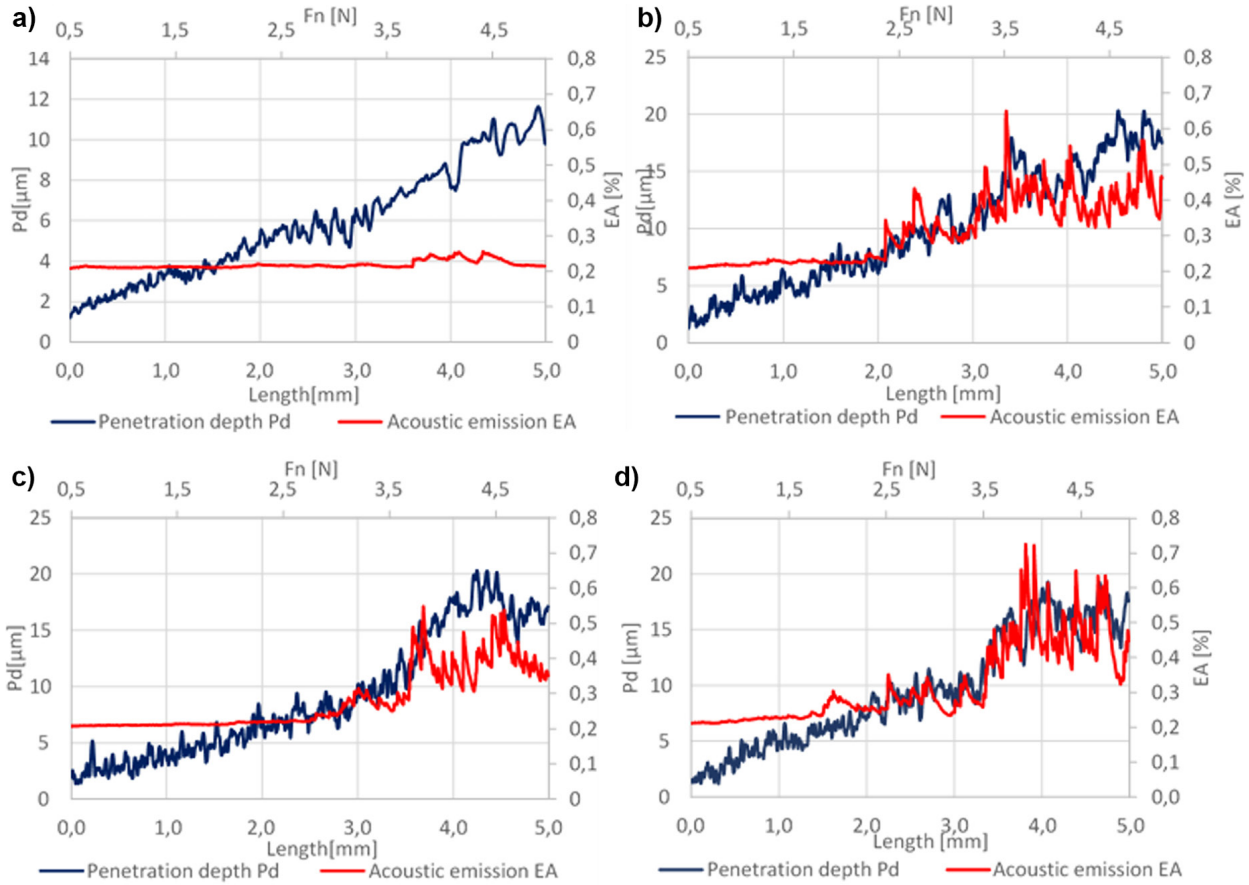

Fig. 7. Acoustic emission curves (EA) and indentation displacement (Pd) recorded during the scratch test as a function of distance and linear load increase (Fn) for sample: a) AZ91, b) PEO SiC, c) PEO BN, d) PEO 10

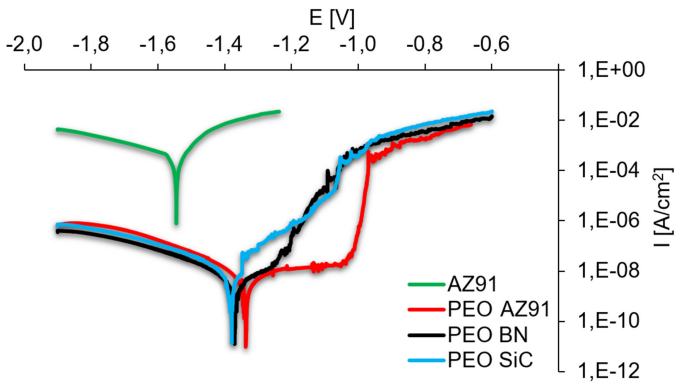

Fig. 8. Potentiodynamic polarization curves of investigated specimens in a 3.5% NaCl solution

while the corrosion current density (*Icorr*) explains the corrosion average rate of the area of the investigated sample. Generally, the lower the *Icorr* value, and the higher the *Ecorr* value, the corrosion resistance of the material is higher. This effect was observed for all samples with PEO coatings compared to the magnesium substrate. This phenomenon is commonly observed and explained by the forming coating and/or the type of introduced particles that have high chemical stability [29-31]. Moreover, it is evident that the curves exhibit similar polarization behavior.

In the anodic polarization curves, no passive regions were observed near the corrosion potential. Moreover, samples with produced PEO coatings were characterized by shifting the cor-

rosion potential to a range of more positive values relative to the base alloy AZ91. Furthermore, the corrosion current of samples after plasma oxidation, regardless of their composition, is almost five orders of magnitude lower compared to the results registered for the unmodified magnesium alloy. However, the polarity resistance of materials after plasma oxidation increased by five orders of magnitude relative to AZ91 (TABLE 3).

TABLE 3

Corrosion parameters of investigated samples

	AZ91	PEO AZ91	PEO BN	PEO SiC
R_{pol} [Ω*cm^2]	71.5	5×10^{6}	10×10^{6}	3.3×10^{6}
Ecorr [V]	–1.54	–1.34	–1.37	–1.38
Icorr [A/cm^2]	4.0×10^{-4}	7.8×10^{-9}	2.6×10^{-9}	1.3×10^{-8}

The registered dependencies indicate increased corrosion resistance of materials with PEO coatings. The lowest corrosion current density and simultaneously the highest polarization resistance value was measured for the PEO BN sample (TABLE 3). These results clearly confirm the highest corrosion resistance in NaCl solution of such a chemical composition of the coating. It was also observed that in the cathode range the potentiodynamic curve of the magnesium alloy is smooth, whereas for all samples with coatings numerous peaks/refractions are visible (Fig. 8). The effect of introducing particles into the electrolyte on the produced PEO coating is not unequivocally explained and tested. Generally, it is postulated that the addition of appropriate particles can increase the corrosion resistance of the substrate made of magnesium or its alloys and improve its abrasion resistance, strength, and hardness [31-34]. However, it depends on many parameters including: method of preparing the substrate, chemical composition of the substrate, zeta potential, particle size, volume fraction of reinforcement, melting point of particles, electrolyte composition, the energy of the discharges [35-37]. The enhancement of materials by the introduction of particles into the coating may also reduce the corrosion resistance of the created layer. Generally, it is a consequence of the loss of homogeneity of the coating as a result of the agglomeration of particles in the coating as a result of incorrectly selected process parameters or too high concentration of the reinforcement introduced into the solution. It has been shown that then numerous micropores can form in the coating, there may be a lack of cohesion between the introduced particle and the matrix or cracks appear on the surface of the coating [38-41]. As a result, they frequently lead to the formation of pitting corrosion.

Such a non-linear shape of curves indicates local loss of PEO coatings and the formation of corrosive cells. Microscopic observations of the areas affected by the 3.5% NaCl solution presented in Fig. 9, confirm the pitting corrosion of PEO coatings.

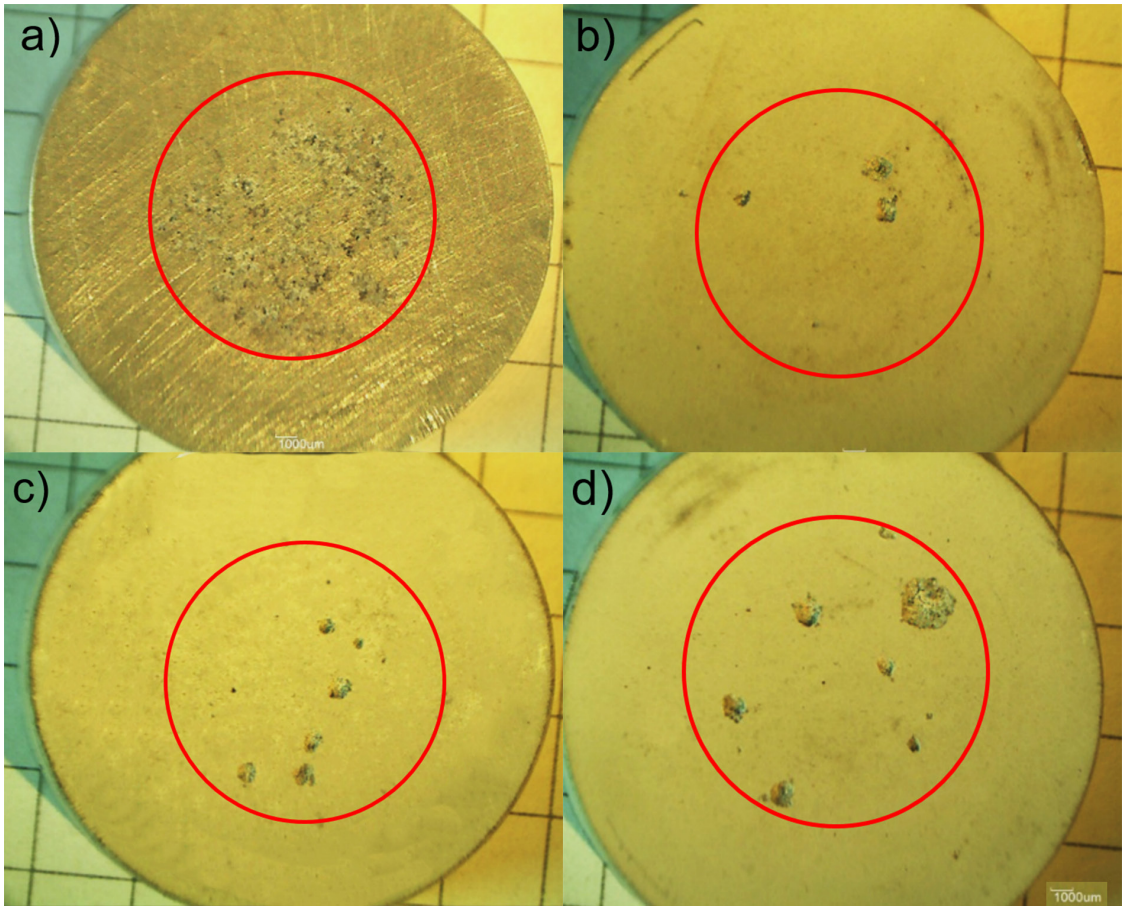

Fig. 9. The surface of samples after potentiodynamic tests in a 3.5% NaCl solution (inside the red circle): a) AZ91, b) PEO BN, c) PEO SiC, d) PEO 10

4. Conclusions

Based on the obtained test results, it was found that among the three analyzed variants of coatings produced on the surface of AZ91 magnesium alloy, the best properties were characterized by layers to which BN was introduced in the PEO process. Such modification allowed obtaining a material with increased: (i) scratch resistance, (ii) microhardness, (iii) corrosion resistance in a 3.5% NaCl solution, and (iv) wear resistance by lowering the coefficient of friction under dry friction conditions – in comparison to the unmodified AZ91 magnesium alloy.

Moreover, all PEO coatings were characterized by a good adhesion-diffusion bond with the substrate and a homogeneous distribution of thickness and roughness.

It was also shown that the type of destruction of PEO coatings, regardless of the type of additive added to them, in a 3.5% NaCl solution has a pitting character.

REFERENCES

[1] Y. Hu, C. Zhang, W. Meng, F. Pan, J.P. Zhou J. Alloys Compd. **727**, 491-500 (2017).

[2] W. Tu, Y. Cheng, X. Wang, T. Zhan, J. Han, Y. Cheng J. Alloys Compd. **725**, 199-216 (2017).

[3] H. Bakhsheshi-Rad, E. Hamzah, M. Kasiri-Asgarani, S.N. Saud, Vacuum **131**, 106-110 (2016).

[4] M.P. Brady, D.N. Leonard, H.M. Meyer III, J.K. Thomson, K.A. Unocic Surf. Coat. Technol. **294**, 164-176 (2016).

[5] Z. Li, Y. Yuan, X. Jing, J. Alloys Compd. **706**, 419-429 (2017).

[6] J. Zhou, J. Xu, S. Huang, Z. Hu, X. Meng, X. Feng Surf. Coat. Technol. **309**, 212-219 (2017).

[7] X. Lu, C. Blawert, K.U. Kainer, M. Zheludkevich Electrochim. Acta. **196**, 680-691 (2016).

[8] F. Simchen, M. Sieber, T. Lampke Surf. Coat. Technol. **315**, 205-213 (2017).

[9] R. Liu, N. Weng, W. Xue, M. Hua, G. Liu, W. Li Surf. Coat. Technol. **269**, 212-219 (2015).

[10] M.P. Kamil, M. Kaseem, Y.H. Lee, Y.G. Ko J. Alloys Compd. **707**, 167-171 (2017).

[11] Y. Gao, A. Yerokhin, E. Parfenov, A. Matthews Electrochem. Acta **149**, 218-230 (2014).

[12] M. Kaseem, M.P. Kamil, Y.G. Ko Surf. Coat. Technol. **322**, 163-173 (2017).

[13] C.J. Wang, F.C. Chang, J.W. Lee, B.S. Lou Surf. Coat. Technol. **303**, 68-77 (2015).

[14] P.H. Sobrinho, Y. Savguira, Q. Ni, S.J. Thorpe Surf. Coat. Technol. **315**, 530-545 (2017).

[15] Y.G. Ko, E.S. Lee, D.H. Shin J. Alloys Compd. **586**, 357-361 (2014).

[16] Y. Chen, Y. Yang, W. Zhang, T. Zhang, F. Wang J. Alloys Compd. **718**, 92-103 (2017).

[17] C. Liu, J. Liang, J. Zhou, Q. Li, Z. Peng, L. Wang Surf. Coat. Technol. **304**, 179-187 (2016).

[18] F. Wei, W. Zhang, T. Zhang, F. Wang J. Alloys Compd. **690**, 195-205 (2017).

[19] L. Shuo-Jen, D.T.H. Le Surf. Coat. Technol. **307**, 781-789 (2016).

[20] M. Sabouri, S.M. Mousavi Khoei Surf. Coat. Technol. **334**, 543-555 (2018).

[21] W. Yang, W. Liu, Z. Peng, B. Liu, J. Liang Ceram. Int. **43**, 16851-16858 (2017).

[22] D.V. Mashtalyar, S.V. Gnedenkov, S.L. Sinebryukhov, I.M. Imshinetskiy, A.V. Puz J. Mater. Sci. Technol. **33**, 461-468 (2017).

[23] L. Bih-Show, L. Yi-Yuan, T. Chuan-Ming, L. Yu-Chu, D. Jenq-Gong, L. Jyh-Wei Surf. Coat. Technol. **332**, 358-367 (2017).

[24] A. Szewczyk-Nykiel, P. Długosz, P. Darłak, M. Hebda J. Mater. Eng. Perform. **26**, 2555-2562 (2017).

[25] R. Arrabal, E. Matykina, T. Hashimoto, P. Skeldon Surf. Coat. Technol. **203**, 2207-2220 (2009).

[26] Y. Song, K. Dong, D. Shan, E.H. Han J. Magnesium Alloy. **1**, 82-87 (2013).

[27] S. Yagi, K. Kuwabara, Y. Fukuta, K. Kubota, E. Matsubara Corros. Sci. **73**, 188-195 (2013).

[28] R.O. Hussein, D.O. Northwood, X. Nie Surf. Coat. Technol. **237**, 357-368 (2013).

[29] K.M. Lee, K.R. Shin, S. Namgung, B. Yoo, D.H. Shin Surf. Coatings Technol. **205**, 3779-3784 (2011).

[30] M. Mohedano, C. Blawert, M.L. Zheludkevich, Elsevier Mater Design, **86**, 735-744 (2015).

[31] A. Fattah-alhosseini, R. Chaharmahali, K. Babaei Journal of Magnesium and Alloys (2020).
DOI: https://doi.org/10.1016/j.jma.2020.05.001.

[32] Y. Lu, C. Jinhui, C. Yingliang Surf. Coat. Tech. **276**, 266-278 (2015).

[33] S. Wan, N. Si, Y. Xia Trans. Nonferrous Met. Soc. China **25**, 1926-1934 (2015).

34] X. Lu, C. Blawert, K. U. Kainer, T. Zhang, F. Wang, M. L. Zheludkevich Surf. Coat. Tech. **352**, 1-14 (2018).

[35] C. Blawert, V. Heitmann, W. Dietzel, H.M. Nykyforchyn, M.D. Klapkiv Surf. Coatings Technol. **201**, 8709-8714 (2007).

[36] L. Yu, J. Cao, Y. Cheng Surf. Coat. Tech. **276**, 266-278 (2015).

[37] J.J. Zhuang, Y.Q. Guo, N. Xiang, Y. Xiong, Q. Hu, R.G. Song Appl. Surf. Sci. **357**, 1463-1471 (2015).

[38] W. Li, M. Tang, L. Zhu, H. Liu, Appl. Surf. Sci. **258**, 10017-10021 (2012).

[39] B. Mingoa, R. Arrabal, M. Mohedano, A. Pardo, E. Matykina Surf. Coat. Tech. **309**, 1023-1032 (2017).

[40] C. Ziejewska, J. Marczyk, A. Szewczyk-Nykiel, M. Nykiel, M. Hebda Adv. Powder Technol. **30**, 835-842 (2019).

[41] J. Zhao, X. Xie, C. Zhang Corros. Sci. **114**, 146-155 (2017).